Rare Metal Materials and Engineering
Volume 49, Issue 11, November 2020
Available online at www.rmme.ac.cn

Science Press

Cite this article as: Rare Metal Materials and Engineering, 2020, 49(11): 3662-3668.

ARTICLE

Micro Strain and Stress Distribution of Phases in Ti-6Al-4V Alloy and Their Influencing Factors

Chen Guoxing[1], Liu Caiyi [2]

[1] School of Mechanical and Electrical Engineering, Hubei Polytechnic University, Huangshi 435003, China; [2] National Engineering Research Center for Equipment and Technology of Cold Strip Rolling, Yanshan University, Qinhuangdao 066004, China

Abstract: A micromechanics finite element (FE) model was established based on the actual microstructure of Ti-6Al-4V alloy. And considering the dual-phase characteristic, the micro-deformation behavior was studied. The results show that the hard transformed β matrix (β_t) bears most external loading force, while the external load deformation is mainly carried out by the soft primary α phase (α_p). With the increase of macro strain, the strain ratio of α_p to β_t and the stress ratio of β_t to α_p are basically unchanged at first, then increase rapidly, and finally remain stable. The volume fraction (f_α) and grain size (d_α) of α_p have an effect on strain and stress distribution in the phases. With the increase of f_α or the decrease of d_α, the strain ratio and stress ratio increase and decrease, respectively.

Key words: Ti-6Al-4V alloy; tension at ambient temperature; micro-deformation; stress ratio; strain ratio

Titanium alloys have many advantages such as high specific strength, corrosion resistance, and low temperature performance. They are widely used in national defense industry and civil industry [1-3]. Titanium alloys have many kinds of microstructures, and the duplex microstructure is widely used due to its excellent performance, which consists of primary α phase (α_p) and transformed β matrix (β_t) at ambient temperature. When the alloy is deformed, the deformation is almost symmetrical at macro level. In fact, the significant discontinuity of the microstructure will result in different deformation behavior at different positions. The deformation behavior is seriously asymmetrical at micro level.

There are some reports on the asymmetrical deformation behavior of titanium alloys. He [4] found that during the deformation of TA15, the plastic deformation is firstly observed in β phase, and the deformation of the constituent phases has coordination problems. This research only qualitatively analyzed the deformation of the phases. Chen et al [5] analyzed the deformation behavior of the constituent phases in titanium alloy during high temperature deformation. But it is assumed that the deformation of each phase is uniform.

With the development of computer and FE technology, it is possible to analyze the micro-deformation of the titanium alloy by FE method. Ankem et al [6, 7] used the triangular elements to establish the FE model of titanium alloy. Neti et al[8, 9] studied the influence of volume fraction and strength ratio of the phases on micro stress and strain localization of the titanium alloy. Tang et al [10] established a FE model based on crystal plastic FE method. Li et al [11] studied the high temperature micro-deformation behavior of Ti-6Al-4V alloy by crystal plastic FE method. The effect of volume fraction, base plane texture strength and grain homogeneity of α phase on deformation compatibility was quantitatively calculated. Shao et al [12] established a FE model based on actual microstructure, and studied the strain and stress distribution in constituent phases, but they did not conduct quantitative researches.

The difference in mechanical properties between α_p and β_t leads to the failure of synchronous deformation. In this work, considering the characteristic of two phases in

Received date: November 14, 2019
Foundation item: Talent Introduction Project of Hubei Polytechnic University (19XJK19R)
Corresponding author: Chen Guoxing, Ph. D., Lecturer, School of Mechanical and Electrical Engineering, Hubei Polytechnic University, Huangshi 435003, P. R. China, E-mail: 201098@hbpu.edu.cn

Ti-6Al-4V alloy, the relationship between microstructure features and macro properties was studied. A micro mechanics FE model was established based on actual microstructure and uniaxial tension conditions. The micro strain and stress distribution of the phases in the alloy during ambient temperature tensile deformation, and the influence of volume fraction (f_α), grain size (d_α) of α_p were quantitatively studied. This study has a certain theoretical significance for better understanding the deformation mechanism, improving the comprehensive mechanical properties, and taking full advantages of titanium alloy.

1 Experiment

The material is an annealed Ti-6Al-4V alloy plate with a thickness of 6 mm. A heat treatment process was designed based on the $(\alpha+\beta)\rightarrow\beta$ phase transition temperature. Firstly, the target alloy was heated to 980 °C and held for 1 h, and then it was heated again to 550 °C and held for 5 h. The heating rate and cooling type for the two heating processes were both 10 °C/s and air cooling. Then, AXIOVERT 200 MAT microscope was used to observe the microstructure, and the result is shown in Fig.1a. The picture is binarized firstly. Then the quantity and area of α_p can be acquired by IMAGE PRO software. Finally, the software can output f_α and d_α, and the results are 11.84% and 10.35 μm, respectively.

The uniaxial tensile test was also carried out on the sample. It was processed into tensile specimens, and INSPEK TABLE 100 electronic universal testing machine was employed to measure the mechanical properties. The tensile speed was set to 1 mm/min, and the gauge length was 44 mm. The strain rate during tension can be calculated, which is 3.79×10^{-4} s^{-1}.

2 Establishment of FE Model

2.1 FE modeling procedure

At ambient temperature, Ti-6Al-4V alloy consists of α_p and β_t. Furthermore, β_t consists of secondary α phase and residual β phase. In order to simplify the model, the secondary α phase and residual β phase are treated as one phase, that is β_t. The volume fraction of β_t in the alloy specimen is relatively high, which is 88.16%. It is considered that β_t is continuous phase, while α_p is embedded phase. In addition, the mechanical properties of the alloy are not only affected by the phases, the interface between the two phases also has a certain contribution to mechanical properties. However, in the study on the contribution of α_p, β_t and α-β interface to the hardness of TA15, it was found that the contribution of α-β interface to the hardness is small, less than 8% [13]. It can be concluded that the effect of interface on mechanical properties is small. And it is neglected when establishing the model in this work.

2.1.1 Geometric modeling and meshing

Firstly, the microstructure is obtained, and the result is shown in Fig.1a. Then, the boundary lines of the phases are recognized and vectorized, as shown in Fig.1b. Finally, the vectorized graphic is optimized and imported into MSC. Marc nonlinear FE software for meshing and setting material plasticity and boundary conditions. The elements of the phases in FE model are shown in Fig.1c.

2.1.2 Stress-strain relationship of constituent phases

The stress-strain curves of the phases at ambient temperature have been established in Ref.[14]. They can be expressed as Eq.(1) and Eq.(2).

$$\sigma=\begin{cases}E\varepsilon_e & \sigma\leqslant\sigma_0\\ \sigma_0+\alpha M\mu b^{\frac{1}{2}}\left[\dfrac{1-\exp(-kM\varepsilon_p)+16f_\alpha k\varepsilon_p}{kd_\alpha}\right]^{\frac{1}{2}} & \sigma>\sigma_0\end{cases} \tag{1}$$

$$\sigma=\begin{cases}E\varepsilon_e & \sigma\leqslant\sigma_0\\ \sigma_0\left(1+\dfrac{E}{\sigma_0}\varepsilon_p\right)^n & \sigma>\sigma_0\end{cases} \tag{2}$$

where σ is the stress, σ_0 is the yield strength; E is the Young's modulus; ε_e and ε_p are the elastic strain and plastic strain, respectively; α, M, μ, b and k are the material constant, Taylor factor, shear modulus, Burger's vector and recovery rate, respectively; n is the strain hardening exponent.

2.1.3 Boundary condition

Periodic boundary conditions are applied in the FE model. Nguyen et al [15] claimed that periodic boundary conditions

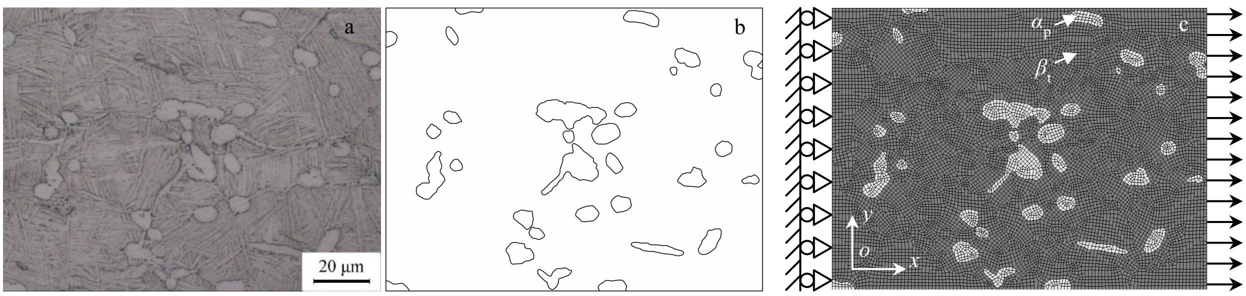

Fig.1 Metallographic microstructures of the heat treated titanium alloy (a), vectorized boundary lines of the model (b), and mesh and boundary condition of the model (c)

can promote the accuracy of the simulated results. As shown in Fig.1c, the nodes on left edge are fixed in x direction, only can move in y direction. The nodes on right edge are controlled by displacement mode in x direction, and the strain rate is 3.79×10^{-4} s^{-1}. And those nodes can move freely in y direction. The nodes on top edge can move synchronously in y direction, without any constraint in x direction. The nodes on bottom edge have the same boundary conditions as those on top edge [16].

2.2 Influence of mesh quantity on results

In order to improve the accuracy and reduce computing time, the simulated stress-strain curves of Ti-6Al-4V alloy based on different mesh quantity are analyzed and compared with experimental result, as shown in Fig.2. There are errors between the simulated and experimental results, but the maximum error is about 12%. When mesh quantity n_E is reduced from 25 367 to 11 531, the error only increases by 0.34%. It can be seen that the mesh quantity has little influence on simulated results. Therefore, in the follow-up simulation, the mesh quantity is controlled at about 12 000.

2.3 Effect of different region microstructures on results

In order to avoid the influence of the microstructure of different positions on the results, five microstructures of different positions in the sample are used to establish the FE models. Fig.3 shows the results of stress-strain curves of the alloy achieved by the models, and comparison with the experimental result. The simulated stress-strain response is almost the same. Although there are errors between the simulated and experimental results, the errors are within acceptable range. It indicates that the size of the model is large enough to contain abundant microstructural characteristics, and the microstructural characteristics of different regions will have no significant effect on the simulation results.

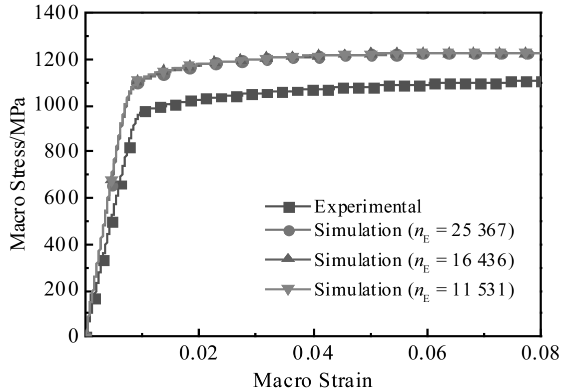

Fig.2 Effect of mesh quantity on simulation results of stress-strain curves for Ti-6Al-4V alloy

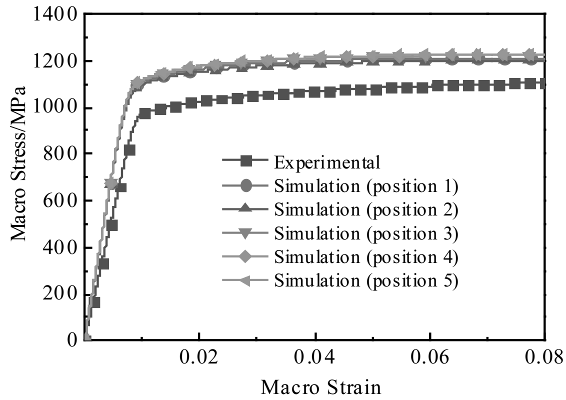

Fig.3 Effect of microstructures in different regions on simulation results of stress-strain curves for Ti-6Al-4V alloy

3 Results and Discussion

3.1 Strain and stress distribution in constituent phases

The strain and stress of different positions are obtained from the simulated result. Then the percentages of different strain and stress ranges are counted. Fig.4a shows the percentage of different strain intervals for the phases when the macro strain are 0.05 and 0.1. When the macro strain is 0.05 and 0.10, the proportion of strain exceeding macro strain in α_p is 86.45% and 87.49%, respectively. While the proportion of strain exceeding macro strain in β_t is 47.74% and 47.88%, respectively. It means that the strain in most regions of α_p is larger than the macro strain, and the strain in more than half of β_t is smaller than the macro strain.

The statistical results indicate that α_p and β_t are soft phase and hard phase in Ti-6Al-4V alloy, respectively. The plastic strain is firstly observed in α_p, and the plastic strain of α_p is greater than that of β_t in the whole macro-deformation process. In addition, even within the same phase, the strains in different positions show greater heterogeneity. Ankem et al [7, 9] studied the deformation behavior of two-phase materials, and significant strain gradient was observed in the interface between the constituent phases, similar to the results found in this study. Yu et al [17] found that ferrite grains in dual phase steel show uneven deformation along tensile direction and other directions, and confirmed the essential characteristics of non-uniform deformation of dual phase materials. Fig.4a also indicates that the β_t participates in strain distribution at low macro strain, which is the same as study of Ghadbeigi et al [18] on the dual-phase steel.

Fig.4b shows the percentage distribution of different stress intervals when macro strain is 0.05 and 0.1. The stress interval of 800~850 MPa possesses the highest percentage in α_p when macro strain are 0.05 and 0.1. While in

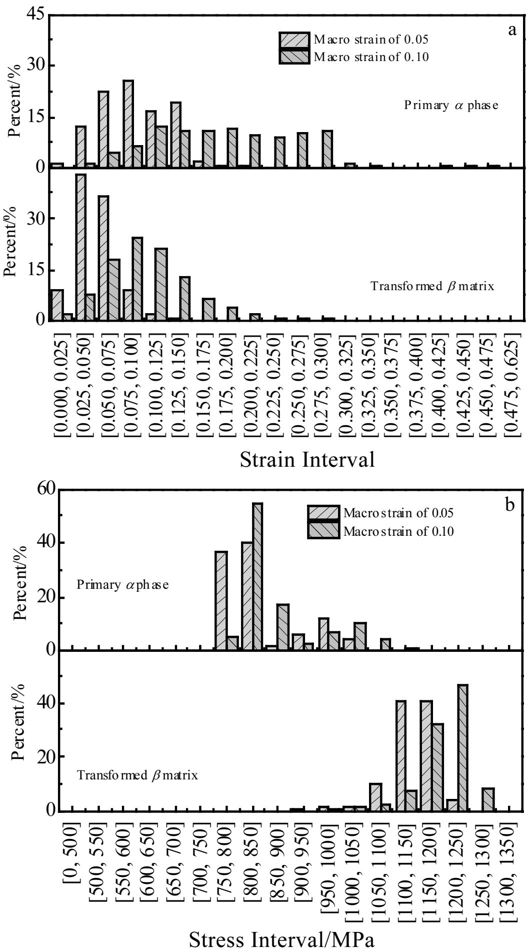

Fig.4 Quantitative statistics for strain distribution (a) and stress distribution (b) in constituent phases

β_t, the stress intervals with the highest percentage at macro strain of 0.05 and 0.10 are 1100~1200 MPa and 1200~1250 MPa, respectively. When macro strain is 0.05, the stress in most regions of α_p exceeds 750 MPa, which is greater than the yield strength. Meanwhile, part of β_t is still in elastic deformation stage. The results show that α_p yields earlier than β_t.

The stress in β_t is greater than that in α_p. Zang [19] and Jinoch [20] et al researched the micro-deformation behavior of Ti-8Mn alloy, and found that the stress localization is firstly observed in soft phase. However, the greatest stress appears in hard phase finally. The deformation inconsistency between α_p and β_t can cause strain and stress interaction between them.

3.2 Strain and stress ratios of constituent phases

The strain ratio between α_p and β_t, stress ratio between β_t and α_p, and the variation curves with macro-strain are demonstrated in Fig.5. The ratios show the same evolution tendency. With the development of macro strain, the strain and stress ratios firstly keep steady, then increase rapidly with the increase of macro strain, and finally remain stable.

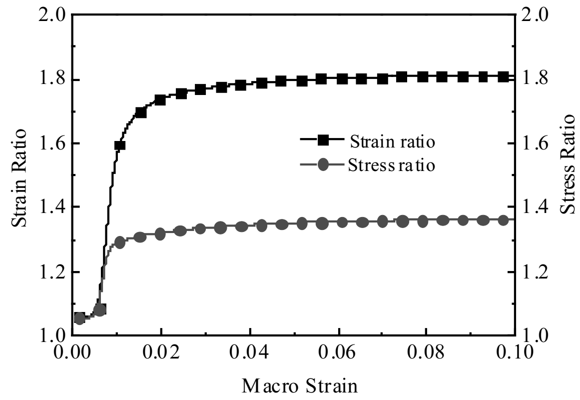

Fig.5 Variation curves of strain and stress ratios with macro strain

The deformation of dual-phase materials can be divided into three stages according to the deformation of constituent phases [21, 22]. Ti-6Al-4V alloy is a two-phase material, and in the first stage, both α_p and β_t are in the stage of elastic deformation. The strain and stress ratios almost keep steady, because the elastic moduli of the phases differ very little. Since α_p and β_t are soft phase and hard phase, respectively, the former assumes more strain and the latter assumes more stress during the deformation. So the strain and stress ratios are both greater than 1. With increase of macro strain, the deformation turns into the second stage. The plastic deformation is observed in α_p, whose strain increases with fast rate, while the flow stress increases less. Since β_t is still in elastic stage, the strain increases slightly but the stress increases rapidly. The strain and stress ratios are rapidly rise. In the third stage, β_t undergoes plastic deformation, and the deformation of the phases is in a relatively stable state. The ratios no longer significantly change, indicating that the deformation coordination between the constituent phases achieves a stable state, but does not mean that the deformation is in a perfect compatible state.

3.3 Influence of f_α on micro-deformation behavior

When alloy elements are fixed, the macro mechanical properties mainly depend on microstructure, such as the volume fraction and grain size of the constituent phases[23, 24]. α_p is duplicated and randomly distributed in β_t on the basis of the original microstructure. The f_α increases to 23.68%, and the average grain size remains the same.

Fig.6 shows the effect of f_α on strain and stress distributions, which is the statistical result when the macro strain is 0.1. f_α has a significant effect on micro deformation behavior.

In Fig.6a, when f_α is 11.84%, the strain distribution difference in range of 0.1~0.3 is small for α_p, showing a significant inhomogeneous deformation behavior. When f_α is 23.68%, the strain of α_p is mainly concentrated in range of 0.125~0.175, and the uneven deformation phenomenon is

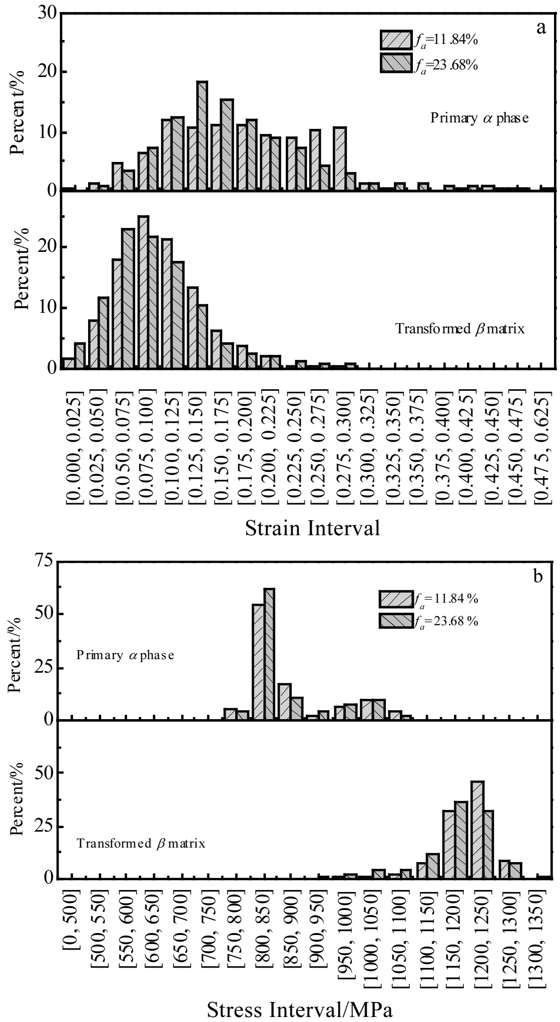

Fig.6 Effect of volume fraction of α_p on strain distribution (a) and stress distribution (b) of constituent phases

improved. In addition, the proportion of strain interval of 0~0.075 in β_t increases as f_α increases from 11.84% to 23.68%, whereas the proportion of strain interval exceeding 0.075 decreases. It indicates that the macro strain assumed in β_t decreases. The same conclusion can be drawn from the quantitative statistical results of stress interval percentage shown in Fig.6b. In α_p, the stress interval of 800~850 MPa wins the maximum percentage whether f_α is 11.84% or 23.68%. But the stress interval percentage of 800~850 MPa increases when f_α increases from 11.84% to 23.68%. It suggests that f_α can promote the uniform deformation. In β_t, the stress intervals of 1200~1250 MPa and 1150~1200 MPa win the maximum percentage when f_α is 11.84% and 23.68%, respectively. The stress of β_t decreases with the increase of f_α.

The effect of f_α on strain and stress ratios is shown in Fig.7. The variation laws of strain and stress ratios with macro strain are not affected by f_α. However, the strain ratio increases and stress ratio decreases with increase of f_α. The strain ratio or stress ratio of each phase is complementary. The previous analysis shows that the strain and stress of β_t decrease relatively when f_α increases. Correspondingly, the strain and stress of α_p increase. Therefore, the strain ratio of α_p to β_t increases, while the stress ratio of β_t to α_p decreases.

3.4 Influence of d_α on micro-deformation behavior

α_p is replicated thrice on the basis of original microstructure, and its length and width are shrunk to $1/\sqrt{2}$ times of the original size. Consequently, f_α and d_α are 23.68% and 7.32 μm, respectively. In addition, the length and width of α_p are enlarged to $\sqrt{2}$ times of the original size. So f_α and d_α are 23.68% and 14.64 μm, respectively.

Fig.8 shows the effect of d_α on strain and stress distribution, which is the statistical result when macro strain is 0.1. d_α also has a significant effect on micro-deformation behavior. In Fig.8a, although the maximum percentage strain interval of α_p is 0.125~0.15 for different d_α, the percentages of different strain intervals vary greatly. The strain of β_t mainly concentrates in small strain interval. The proportion of large strain intervals increases significantly as d_α increases. When d_α is 7.32, 10.35, and 14.64 μm, the strain intervals with high proportion are 0.025~0.1, 0.05~0.125 and 0.075~0.125, respectively. As shown in Fig.8b, the stress interval of 800~850 MPa wins the largest proportion in α_p, but the proportion of this stress interval increases significantly with increase of d_α. While the proportions of other stress intervals are very small in α_p. The stress distribution of β_t is mainly concentrated in 1150~1250 MPa, but the percentage of each stress interval varies significantly when d_α changes.

The effects of α_p grain size on strain and stress ratios are shown in Fig.9. The variation laws of the strain and stress ratios with the macro strain are not affected by the grain size. As the grain size increases, the strain ratio decreases and the stress ratio increases.

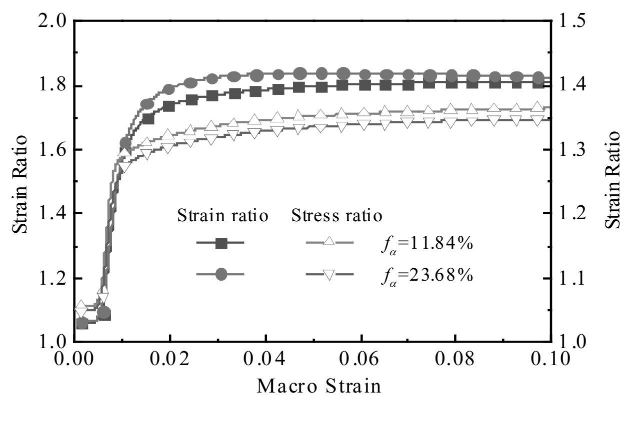

Fig.7 Effect of volume fraction of α_p on strain and stress ratios

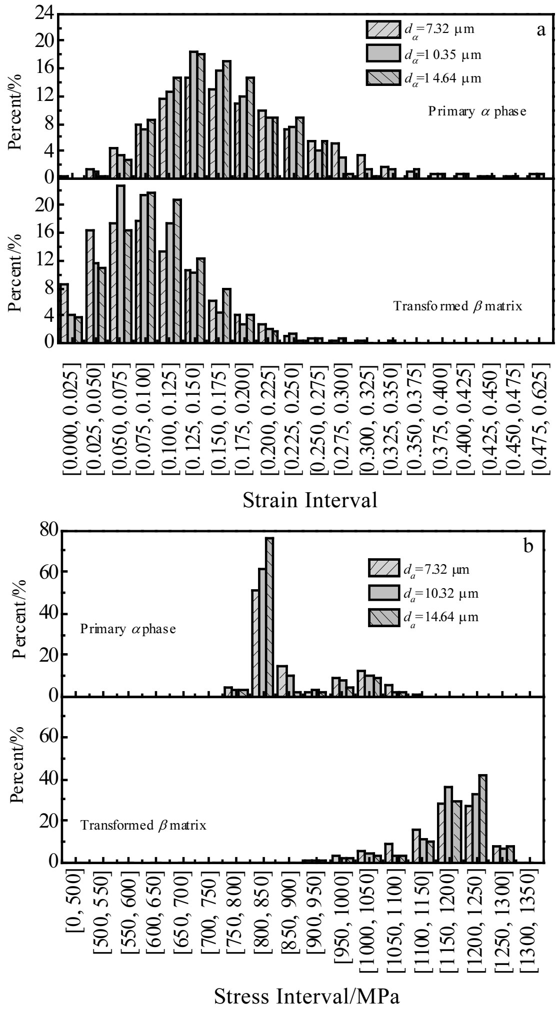

Fig.8 Effect of α_p grain size on train (a) and stress (b) distributions

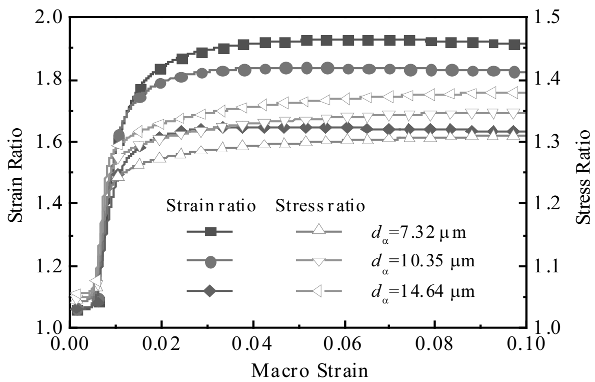

Fig.9 Effect of α_p grain size on strain and stress ratios

4 Conclusions

1) The strain and stress distribution in the constituent phases of Ti-6Al-4V alloy are greatly different during deformation.

2) The strain and stress ratios firstly keep steady, then increase rapidly, and finally remain stable, indicating that the deformation coordination between the constituent phases achieves a stable state.

3) With the increase of f_α, the asymmetrical deformation behavior of α_p is improved, while the deformation degree and stress of β_t are reduced.

4) The proportion of each strain and stress interval of the phases varies significantly with the change of grain size. With the increase of the grain size, the strain ratio decreases and stress ratio increases.

References

1 Liu Q M, Zhang C H, Liu S F *et al*. *Journal of Iron and Steel Research*[J], 2015, 27(3): 1 (in Chinese)

2 Chang H, Wang X D, Zhou L. *Materials China*[J], 2014(S1): 603 (in Chinese)

3 Zhu Z S. *Aviation Industry Press*[M]. Beijing: Aviation Industry Press, 2013 (in Chinese)

4 He D. *Dissertation for Doctorate*[D], Harbin: Harbin Institute of Technology, 2012 (in Chinese)

5 Chen G X, Peng Y. *Journal of Plasticity Engineering*[J], 2017, 24(5): 107 (in Chinese)

6 Ankem S, Margolin H. *Metallurgical Transactions A*[J], 1982, 13(4): 595

7 Ankem S, Margolin H. *Metallurgical Transactions A*[J], 1982, 13(4): 603

8 Neti S, Vijayshankar M N, Ankem S. *Materials Science and Engineering A*[J], 1991, 145(1): 47

9 Neti S, Vijayshankar M N, Ankem S. *Materials Science and Engineering A*[J], 1991, 145(1): 55

10 Tang B, Xie S, Liu Y *et al*. *Rare Metal Materials and Engineering*[J], 2015, 44(3): 532

11 Li X X, Zhang, J H, Xu D S *et al*. *The Sixteenth National Conference on Titanium and Titanium Alloys*[C]. Xi'an: China Nonferrous Metals Industry Association, 2016 (in Chinese)

12 Shao J B, Zhang X C, Wang Y *et al*. *Materials for Mechanical Engineering*[J], 2016, 40(2): 102 (in Chinese)

13 Ji Z, Yang H, Li H W. *Materials and Design*[J], 2015, 87: 171

14 Chen G X, Peng Y, Shi B D *et al*. *Metallurgical Research and Technology*[J], 2017, 114(4): 408

15 Nguyen V D, Béchet E, Geuzaine C *et al*. *Computational Materials Science*[J], 2012, 55: 390

16 Choi K S, Liu W N, Sun X *et al*. *Acta Materialia*[J], 2009, 57(8): 2592

17 Yu Z Z, Barabash R, Barabash O *et al*. *JOM*[J], 2013, 65(1): 21

18 Ghadbeigi H, Pinna C, Celotto S *et al*. *Materials Science & Engineering A*[J], 2010, 527(18-19): 5026

19 Zang X L, Zhao X Q, Park J *et al*. *Rare Metal Materials and Engineering*[J], 2009, 38(6): 1058 (in Chinese)

20 Jinoch J, Ankem S, Margolin H. *Materials Science and Engineering*[J], 1978, 34(3): 203

21 Dong Y, Jia Y Q, Xu L H. *Journal of Hebei University of Technology*[J], 2000, 29(1): 67 (in Chinese)
22 Bag A, Ray K K, Dwarakadasa E S. *Metallurgical and Materials Transactions A*[J], 1999, 30(5): 1193
23 Ramazani A, Mukherjee K, Schwedt A *et al*. *International Journal of Plasticity*[J], 2013, 43: 128
24 Ramazani A, Mukherjee K, Prahl U *et al*. *Metallurgical and Materials Transactions A*[J], 2012, 43A(10): 3850

Ti-6Al-4V 合金组成相的微观应力应变分布及影响因素

陈国兴[1]，刘才溢[2]
(1. 湖北理工学院 机电工程学院，湖北 黄石 435003)
(2. 燕山大学 国家冷轧板带装备及工艺工程技术研究中心，河北 秦皇岛 066004)

摘　要：基于真实组织图像建立了 Ti-6Al-4V 合金的微观力学有限元模型，考虑双相特征研究了合金的微观变形行为。结果表明：外部加载力主要由较硬的 β 转变组织承担，而塑性变形主要由较软的初生 α 相承担。随宏观应变增大，初生 α 相与 β 转变组织的应变比、β 转变组织与初生 α 相应力比首先基本保持不变，而后迅速增大，最后保持稳定。初生 α 相的体积分数和晶粒尺寸对组成相内部的应变和应力分布有影响，随体积分数增大或晶粒尺寸减小，应变比和应力比分别增大和减小。

关键词：Ti-6Al-4V合金；室温拉伸；微观变形；应力比；应变比

作者简介：陈国兴，男，1990 年生，博士，讲师，湖北理工学院机电工程学院，湖北 黄石 435003, E-mail: 201098@hbpu.edu.cn